ORIGINAL ARTICLE

Glycinamide Facilitates Nanocomplex Formation and Functions Synergistically with Bone Morphogenetic Protein 2 to Promote Osteoblast Differentiation *In Vitro* and Bone Regeneration in a Mouse Calvarial Defect Model

Sang-Hyeon Nam[1] · Ju Ang Kim[1] · Soomin Lim[1] · Su Jeong Lee[1] ·
Chun-Ho Kim[2] · Jong-Sup Bae[3] · Yong Chool Boo[4] · Young-Jin Kim[5] ·
Eui Kyun Park[1]

Abstract

BACKGROUND: This study aimed to identify glycine analogs conducive to the formation of cell-absorbable nanocomplexes, enhancing collagen synthesis and subsequent osteogenesis in combination with BMP2 for improved bone regeneration.

METHODS: Glycine and its derivatives were assessed for their effects on osteogenic differentiation in MC3T3-E1 cells and human bone marrow mesenchymal stem cells (BMSCs) under osteogenic conditions or with BMP2. Osteogenic differentiation was assessed through alkaline phosphatase staining and real-time quantitative polymerase chain reaction (RT-qPCR). Nanocomplex formation was examined via scanning electron microscopy, circular dichroism, and ultraviolet–visible spectroscopy. *In vivo* osteogenic effects were validated using a mouse calvarial defect model, and bone regeneration was evaluated through micro-computed tomography and histomorphometric analysis.

RESULTS: Glycine, glycine methyl ester, and glycinamide significantly enhanced collagen synthesis and ALP activity in conjunction with an osteogenic medium (OSM). GA emerged as the most effective inducer of osteoblast differentiation marker genes. Combining GA with BMP2 synergistically stimulated ALP activity and the expression of osteoblast markers in both cell lines. GA readily formed nanocomplexes, facilitating cellular uptake through strong electrostatic interactions. In an *in vivo* calvarial defect mouse model, the GA and BMP2 combination demonstrated enhanced bone volume, bone volume/tissue volume ratio, trabecular numbers, and mature bone formation compared to other combinations.

CONCLUSION: GA and BMP2 synergistically promoted *in vitro* osteoblast differentiation and *in vivo* bone regeneration through nanocomplex formation. This combination holds therapeutic promise for individuals with bone defects, showcasing its potential for clinical intervention.

Keywords Bone morphogenetic protein 2 · Glycinamide HCl · Bone regeneration

Sang-Hyeon Nam and Ju Ang Kim are equally contributed to this work.

✉ Young-Jin Kim
yjkim@cu.ac.kr

✉ Eui Kyun Park
epark@knu.ac.kr

[1] Department of Oral Pathology and Regenerative Medicine, School of Dentistry, Institute for Hard Tissue and Bio-Tooth Regeneration, Kyungpook National University, Daegu 41940, Republic of Korea

[2] Laboratory of Tissue Engineering, Korea Institute of Radiological and Medical Sciences, Seoul 01812, Republic of Korea

[3] College of Pharmacy, Research Institute of Pharmaceutical Sciences, Kyungpook National University, Daegu 41566, Republic of Korea

[4] Department of Molecular Medicine, School of Medicine, Kyungpook National University, Daegu 41944, Republic of Korea

[5] Department of Biomedical Engineering, Daegu Catholic University, Gyeongsan 38430, Republic of Korea

1 Introduction

Bone morphogenetic protein 2 (BMP2) is widely used for treating fractures and in spine fusion surgery. However, applying high dosages of BMP2 can cause a range of serious clinical adverse effects, including cervical spine swelling, inflammation, ectopic bone formation, bone resorption, inadequate adipogenesis, and the potential development of tumors [1, 2]. These adverse effects of BMP2 are primarily associated with the use of a supraphysiological dosage of BMP2, and significant efforts have been made to minimize the potential risks associated with such dosages. One strategy to mitigate these effects is to employ combination therapies with BMP2. In particular, using endogenous metabolites or component molecules that naturally occur in the body and exhibit synergistic effects with BMP2 can reduce the required dosage of BMP2 and alleviate side effects.

Osteogenesis involves the synthesis and secretion of extracellular matrix (ECM) proteins followed by deposition of calcium phosphate minerals. Collagen type I (COL1) accounts for 90% of the ECM in the skeletal tissue [3] and provides the framework for structural and functional integrity of the tissue. It promotes the differentiation of osteoprogenitors or mesenchymal stem cells into osteoblasts [4–6]. Optimal collagen deposition is important during bone defect repair [7], and the major amino acids found in collagen or their derivatives required for collagen biosynthesis may consequently affect osteoblast differentiation and bone regeneration.

Amino acids, particularly glycine, proline, and lysine, are important components of collagen chains, triple helix formation [8], and biosynthesis during osteogenesis [9–11]. Proline and lysine hydroxylation is critical for regulating collagen self-assembly into functional ECM [8]. Lysine favorably influences osteogenesis of bone marrow cells cultured on hydroxyapatite scaffolds [12]. Additionally, the osteogenic response of human mesenchymal stem cells on silk scaffolds with different crystallinities is directly linked to cellular utilization of lysine and proline [13]. Glycine is the most abundant amino acid and found as approximately every third residue in fibrillar collagen [14]. Glycine increases the synthesis of collagen in chondrocytes [15] and enhances the differentiation of osteoclast-like MG63 cells into osteoblasts [16]. Moreover, glycine oral administration significantly increases alkaline phosphatase (ALP) activity and enhances bone mineral density, trabecular number, and connectivity density in ovariectomized mice [16]. Several amidated amino acids and derivatives are known to be effective against hyperpigmentation through the reduction of melanin production in the skin [17, 18]. In particular, the combination of glycinamide (GA) and

ascorbic acid synergistically promotes collagen production and wound healing in human dermal fibroblasts [19]. Recently, dimethyloxallyl glycine (DMOG), a glycine derivative-containing scaffold, was shown to induce angiogenesis and osteogenesis [20]. Functional regeneration of periodontal tissue was induced using a DMOG/nanosilicate-loaded osteogenic/angiogenic difunctional fibrous structure [21]. DMOG had a synergistic effect with BMP2 during the repair of a rat bone defect model by significantly increasing collagen expression at both the mRNA and protein levels in human bone marrow mesenchymal stem cells (BMSCs) [22]. Thus, the synergistic effects of BMP2 with other compounds may be due to the enhanced activation of BMP2 signaling pathways or formation of nanocomplexes.

Various biocompatible nanocomplexes can promote intracellular uptake of drugs or proteins into target sites [23, 24], and polymeric micelles and nanoparticles have been extensively investigated for delivering drugs or proteins. Charged compounds are prone to form nanocomplexes with proteins, and consequently, glycine and its derivatives may have the potential to form nanocomplexes to stimulate collagen biosynthesis and osteoblast differentiation and thereby promote bone regeneration.

Therefore, to identify candidates that can effectively strengthen the therapeutic efficacy of BMP2 used in bone regeneration clinical therapy, we screened glycine derivatives and found that GA has a synergistic effect with BMP2 on *in vitro* osteoblast differentiation and *in vivo* calvarial bone regeneration. Additionally, the mechanism behind how GA produces a synergistic effect with BMP2 was evaluated.

2 Materials and methods

2.1 Cell culture and reagents

MC3T3-E1 cells were cultured with minimum essential medium Eagle-alpha modification (α-MEM) without ascorbic acid (Welgene, Gyeongsan, Korea) with 10% fetal bovine serum (FBS) and 1% penicillin/streptomycin (P/S) [25]. Human BMSCs obtained from Lonza (PT-2501) were cultured in α-MEM supplemented with 10% FBS and 1% P/S. For inducing osteoblast differentiation of human BMSCs, an osteogenic medium (OSM) containing 10 mM β-glycerophosphate, 50 μg/mL ascorbic acid, and 10 nM dexamethasone in growth media was used. Glycine derivatives were dissolved in water to a concentration of 1 M. Recombinant human BMP2 was purchased from Cowellmedi (Busan, Korea).

2.2 Cell viability and proliferation

The 3-(4,5-dimethylthiazol-2-yl)-2,5-diphenyltetrazolium bromide (MTT) (Sigma–Aldrich, St. Louis, MO, USA) assay was used to examine the cytotoxicity of glycine and its derivatives in MC3T3-E1 cells and human BMSCs. Cells were seeded in a 96-well plate at 7×10^3 (MC3T3-E1 cells) or 7×10^2 (human BMSCs) cells per well and incubated overnight. Cells were then treated with α-MEM containing 10% FBS with or without glycine or its derivatives at the indicated concentrations for 24 and 72 h. After the indicated times, cells were incubated with 5 μg/mL MTT for 2 h, and insoluble formazan was dissolved in 100 μL of dimethyl sulfoxide. The absorbance at 570 nm was measured using a microplate reader (Epoch; BioTek Instruments, Winooski, VT, USA). The experiment was repeated thrice, and cell proliferation inhibition was expressed as a relative fold change value for vehicle-treated cells.

2.3 ALP assay

ALP staining was performed to examine the effect of glycine derivatives on ALP activity of MC3T3-E1 cells. Cells were seeded in a 48-well plate at 5×10^4 cells per well and then treated with growth media (normal condition) with or without glycine derivatives and BMP2. Culture media were replaced every 3 days. After 6 days, cells were washed with phosphate-buffered saline (PBS) and fixed with citrate–acetone–formaldehyde fixation solution for 30 s. A staining solution was prepared by combining sodium nitrite solution, FRV-Alkaline solution, distilled water, and naphthol AS-BI alkaline solution at a ratio of 1:1:45:1 as follows: sodium nitrite and FRV-Alkaline solutions were placed in a conical tube and reacted at room temperature for 2 min. Then, distilled water and naphthol AS-BI alkaline solution were added and mixed. Fixed cells were washed with distilled water after removing the fixative, and then the distilled water was removed. The ALP reaction reagent prepared above was added to each well and reacted for 15 min at room temperature in the dark. Stained cells were washed twice with distilled water and then imaged using a BX41 microscope (Olympus, Tokyo, Japan).

2.4 Alizarin red S staining and trichrome staining

Alizarin Red S staining was performed to evaluate the effect of glycine and GA on mineralization of human BMSCs. Human BMSCs were seeded in a 48-well plate at 1×10^4 cells per well and stabilized in a CO_2 incubator for 1 day. Cells were treated with OSM for 3 days, and then media were replaced with OSM and 50 ng/mL of BMP2 with or without glycine or GA. Culture media were replaced every 3 days. After 21 days, cells were washed with PBS and fixed with 70% ethanol for 10 min. Before staining, cells were rinsed once with distilled water. Alizarin Red S staining solution was added to the cells and allowed to react for 10 min at room temperature. The Alizarin Red S staining solution was then removed, and cells washed 2–3 times with distilled water. The Alizarin Red S-stained cells were imaged using a BX41 microscope (Olympus, Tokyo, Japan). Cetylpyridinium chloride (CPC) extraction was performed to quantify the mineralization of human BMSCs. CPC solution (10%) was added to Alizarin Red S-stained wells at 200 μL per well and incubated at room temperature for 2 h. The extracted solution was then diluted five-fold, and absorbance was measured at 570 nm using a microplate reader. Collagen staining was performed using Masson's trichrome stain kit (Polyscience, Inc. PA, USA) by manufacturer' instructions.

2.5 RT-qPCR

Total RNA from cells was isolated using TRI-Solution^{TM} (Bio Science Technology, Seoul, Korea). Isolated RNA (1 μg) was reverse transcribed using SuperiorScript II Reverse Transcriptase (Enzynomics, Korea), and cDNA was synthesized with Oligo(dT)$_{15}$ primer (Promega, Madison, WI, USA). cDNA (2 μL) was amplified via real-time quantitative polymerase chain reaction (RT-qPCR) with the mouse and human primers (Supplementary Table 1). The cDNA was used for RT-qPCR analyses using TB Green Premix Ex Taq II (Tli RNaseH Plus) (Takara Bio Inc., Shiga, Japan) and LightCycler 1.5 (Roche, Basel, Switzerland). Crossing threshold values for individual genes were normalized to *GAPDH* expression.

2.6 Immunocytochemistry

Immunocytochemistry was performed to investigate the effect of glycine and GA on collagen production and deposition in human BMSCs. Human BMSCs were seeded on 12-mm coverslips (SPL Life sciences, Korea) in a 24-well-plate at 2×10^4 cells per well and stabilized in a CO_2 incubator for 1 day. Cells were treated with OSM for 3 days and then 50 ng/mL of BMP2 with or without 0.5 or 1 mM of glycine or GA. Media were changed every 3 days. After 7 days, cells were washed with PBS and fixed with 4% paraformaldehyde for 1 h at room temperature. After washing thrice with PBS for 5 min each, blocking was performed with 5% normal goat serum (NGS) in PBS at room temperature for 1 h. ColI monoclonal antibody (Invitrogen, MA1-26771) diluted 1:200 in 2.5% NGS and 0.25% Triton X-100 in PBS was added, and cells were incubated at 4 °C overnight. Subsequently, cells were

washed thrice with PBS for 5 min each. Later, the cells were treated with goat anti-mouse immunoglobulin G (IgG) (Superclonal™ Recombinant Secondary Antibody, Alexa Fluor™ 488, Invitrogen, A28175) diluted 1:500 in 2.5% NGS and 0.25% Triton X-100 in PBS and incubated at room temperature for 2 h in the dark. The cells were then washed with PBS for 5 min and treated with 4′,6-di-amidino-2-phenylindole dihydrochloride (DAPI; Santa Cruz Biotechnology, Santa Cruz, CA, USA) diluted 1:500 in PBS at room temperature for 2 min in the dark. There-after, the cells were washed thrice with PBS for 5 min each, and finally with distilled water, and then mounted with fluorescence mounting medium (Dako Agilent, Santa Clara, CA, USA). Stained cell images were acquired using a Leica DM 2500 fluorescence microscope (Leica Microsystems, Wetzlar, Germany).

2.7 Immunoblotting

Western blotting was performed to examine the effect of glycine and GA on protein expression. Human BMSCs were seeded at 2×10^5 cells/dish in a 60-mm dish, and cells were allowed to settle for 24 h at 37 °C in a CO_2 incubator. Cells were treated with OSM for 3 days, and then OSM with 50 ng/mL of BMP2 and 0.5 or 1 mM glycine or GA for 4 days. To measure the protein expres-sion of COL1 and bone sialoprotein (BSP), whole cell lysates were extracted with PRO-PREP Protein Extraction Solution (iNtRON Biotechnology, Seongnam-Si, Korea). Whole cell lysates (20 μg) were separated via 7.5% sodium dodecyl sulfate–polyacrylamide gel electrophoresis and then transferred onto nitrocellulose membranes. Mem-branes were incubated overnight with COL1 or BSP anti-body (Cell Signaling Technology, Danvers, MA, USA). Protein bands were detected using horseradish peroxidase-conjugated secondary antibodies, visualized with Western-nBright™ enhanced chemiluminescence (ECL) horse-radish peroxidase (HRP) Substrate (Advansta, San Jose, CA, USA), and imaged using Azure c600 (Azure Biosys-tems, Dublin, CA, USA). COL1 and BSP band expression was normalized to β-actin expression.

2.8 Nanocomplex measurements

To assess the formation of nanocomplexes, 3 mg/mL GA was mixed with 1 mg/mL bovine serum albumin (BSA) and incubated at 37 °C for 4 h. Nanocomplexes were iso-lated via centrifugation at $10,000 \times g$ and washed twice with PBS. Subsequently, 3 mg of nanocomplexes was resuspended in 3 mL of PBS for further characterization. The surface morphology of nanocomplexes was observed via scanning electronic microscopy (SEM, Mira III, TES-CAN, Czech Republic) after sputter-coating the samples

with platinum. Circular dichroism (CD) spectra were recorded on a Jasco J-1500 spectrophotometer (Tokyo, Japan) at 25 °C under a nitrogen flow of 5 mL/min. Changes in the UV–visible (UV–Vis) spectrum of BSA (1 mg/mL) with the addition of GA (1 − 5 mg/mL) were measured using a Hitachi U-2900 spectrometer (Tokyo, Japan).

2.9 Animal experiments

Six-week-old male ICR mice were purchased from Dae Han Bio Link (Chungbuk, Korea) and housed in a con-trolled atmosphere (24 °C ± 1 °C at 50% relative humid-ity) under a 12 h light/12 h dark cycle with free access to a standard diet (Dae Han Bio Link) and sterile tap water. After a 1-week acclimatization period, mice were ran-domly grouped as follows: collagen sponge with vehicle (n = 4), collagen sponge with 1 M glycine (n = 4), colla-gen sponge with 1 M GA (n = 4), collagen sponge with 0.25 μg BMP2 (n = 4), collagen sponge with 0.25 μg BMP2 and 1 M glycine (n = 5), and collagen sponge with 0.25 μg BMP2 and 1 M GA (n = 4). Mice were anes-thetized with a mixture of tribromoethanol (Avertin) and 2-methyl-2-butanol. The calvarial site was shaved, and the skin and periosteum were opened with a scalpel; a 2-mm-sized defect was induced from both parietal bones using a Trephine bur (MCTBIO, Yongin, Korea) and dental handpiece (Surgic XT, Nakanishi, Japan). Then, 2-mm-diameter absorbable collagen sponges (CollaTape®, Inte-gra Lifesciences Corporation, Princeton, NJ, USA) were transplanted into the defect. Collagen sponges used for surgery were soaked in 0.25 μg/0.5 μL BMP2 and 2 M/0.5 μL glycine or GA to a final concentration of 0.25 μg BMP2 and 1 M glycine or GA. After transplantation, the periosteum and skin were closed, and suture was performed using suture 7–0 (AILEE Co., Busan, Korea). The study protocol was reviewed by the Committee on the Care and Use of Animals in Research at Kyungpook National University (KNU 2021–0071).

2.10 Micro-computed tomography (micro-CT) and histological analysis

The calvarial bones were fixed in 10% buffered formalin for 1 day at room temperature and washed with PBS thrice. Nonessential parts were removed and scanned using a SkyScan 1272 high-resolution micro-CT system (Bruker, Kontich, Belgium) with a 70-kV source voltage, 142-μA current, and 10-μm resolution. The region of interest was designated as 2-mm in diameter and 0.5-mm in height for assessing the new bone formation on the calvarial defect site; three-dimensional images of the new bone formation were acquired using CTvox software. Before embedding,

samples were decalcified with 0.5 M ethylenediaminete-traacetic acid (EDTA) for 2 weeks at 4 °C. Samples were then paraffinized and sectioned. For histological analysis, hematoxylin & eosin (H&E) and Masson's trichrome (VitroView™ Masson's Trichrome Stain Kit; VitroVivo Biotech, Rockville, MD, USA) staining were performed. Images were obtained using a DM 2500 microscope (Leica Biosystems Richmond Inc., Richmond, IL, USA). Bone area percentage was quantified in H&E-stained images using iSolution software (Daejeon, Korea), and new bone and mature bone percentages in trichrome-stained samples were quantified using ImageJ (National Institutes of Health, Bethesda, MD, USA).

2.11 Statistical analysis

Data are presented as the mean ± standard error of the mean. All experiments were performed in triplicate. Statistical significance was analyzed using GraphPad Prism 4.0 (GraphPad Software Inc., San Diego, CA, USA) through one-way analysis of variance (ANOVA) with Bonferroni multiple comparison post-tests or Student's t test.

3 Results

3.1 Identification of osteogenic *glycine* derivatives in MC3T3-E1 cells

Glycine can stimulate osteoblast differentiation and protect ovariectomy-induced bone loss [16]. We screened several glycine derivatives to identify a glycine derivative harboring a greater osteogenic potential than that of glycine. MC3T3-E1 cells were treated with 1 mM glycine or glycine derivatives, including glycylglycine (GG), glycine methyl ester (GM), acetyl glycine (AG), acetyl glycinamide (AGA), and GA in the presence of OSM, and collagen deposition and the expression of osteoblast differentiation marker genes were analyzed by trichrome staining and RT-qPCR, respectively. Glycine stimulated deposition of collagen (blue color, Fig. 1A). Moreover, collagen deposition was more enhanced by GG, AG, AGA, and GA than by glycine (Fig. 1A). Glycine, GG, GM, AG, and GA significantly induced the expression of *Col1a1*, confirming that glycine derivatives stimulate collagen expression and deposition. The expression of osteoblast differentiation-related genes was also induced by the glycine derivatives (Fig. 1B), and GM and GA strongly induced the expression of *Alp*, *Osx*, *Runx2*, and *Ocn* (Fig. 1B). Thus, the glycine derivatives GM and GA may induce collagen deposition and osteoblast differentiation.

We then examined the cooperative effects of glycine derivatives and BMP2 on osteoblast differentiation of MC3T3-E1 cells. ALP activity and osteoblast differentiation marker gene expression were analyzed in cells treated with 50 ng/mL of BMP2 with or without glycine derivatives. ALP activity was found to be higher in cells treated with glycine, GM, AG, and GA in the presence of BMP2 at day 6 than in cells treated with BMP2 alone (vehicle) (Fig. 2A). Moreover, glycine, GM, and GA in combination with BMP2 induced the expression of osteoblast marker genes. Most of the glycine derivatives induced the expression of *Col1a1*, *Alp*, *Osx*, and *Runx2*, and the highest induction of expression (2.75-, 2.94-, 6.3-, 2.67-, and 4.88-fold, respectively) was achieved with GA combined with BMP2 when compared with BMP2 alone (vehicle) (Fig. 2B). In particular, the expression of *Col1a1*, *Alp*, *Osx*, and *Bsp* induced by BMP2 plus GA was significantly increased by 76, 52.1, 102.7, and 253.6%, respectively, compared with that induced by BMP2 plus glycine (Fig. 2B). Analysis of the effects of glycine and GA on the cytotoxicity and proliferation of cells showed that GA partially retarded the proliferation of MC3T3-E1 cells and human BMSCs on day 3 but did not cause a cytotoxic effect on day 1 (Fig. 2C, D). These results suggest that among glycine derivatives, GA synthesized collagen most effectively and stimulated osteoblast differentiation in mouse cells.

3.2 Cooperative induction of osteoblast differentiation by GA and BMP2 in human BMSCs

Osteogenic factors found in murine or murine-derived cells do not always exhibit the same responses found in human or human-derived cells, and we therefore examined whether GA has similar osteogenic effects on human cells. Human BMSCs were treated with BMP2 and OSM in combination with glycine or GA, and mineralization (assessed via Alizarin Red S staining) and osteoblast differentiation maker gene expression were analyzed. In combination with BMP2, glycine at 0.5 and 1 mM (Fig. 3Aii, iii) increased calcium deposition in a concentration-dependent manner compared with BMP2 alone (Fig. 3Ai). GA at 0.5 and 1 mM (Fig. 3Aiv, v) in combination with BMP2 also increased calcium deposition in a concentration-dependent manner compared with BMP2 alone or with BMP2 plus glycine. GA showed the strongest calcium deposition (Fig. 3Aiv and v). Quantification of staining with CPC extraction showed that GA plus BMP2 was 3.9- and 5.02- fold higher at 0.5 and 1 mM, respectively, than that of BMP2 alone (Fig. 3B). RT-qPCR was used to assess the osteogenic effect of glycine and GA on the expression of osteoblast differentiation marker genes.
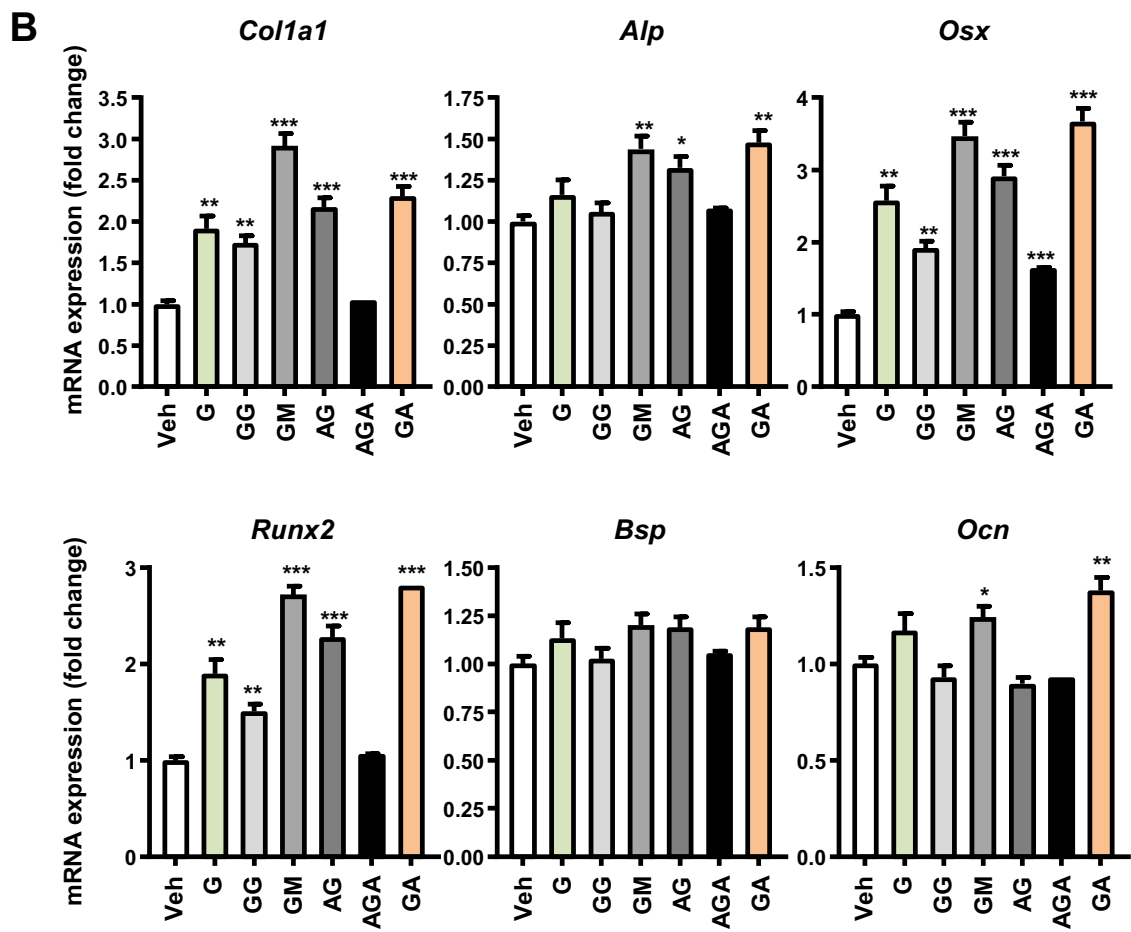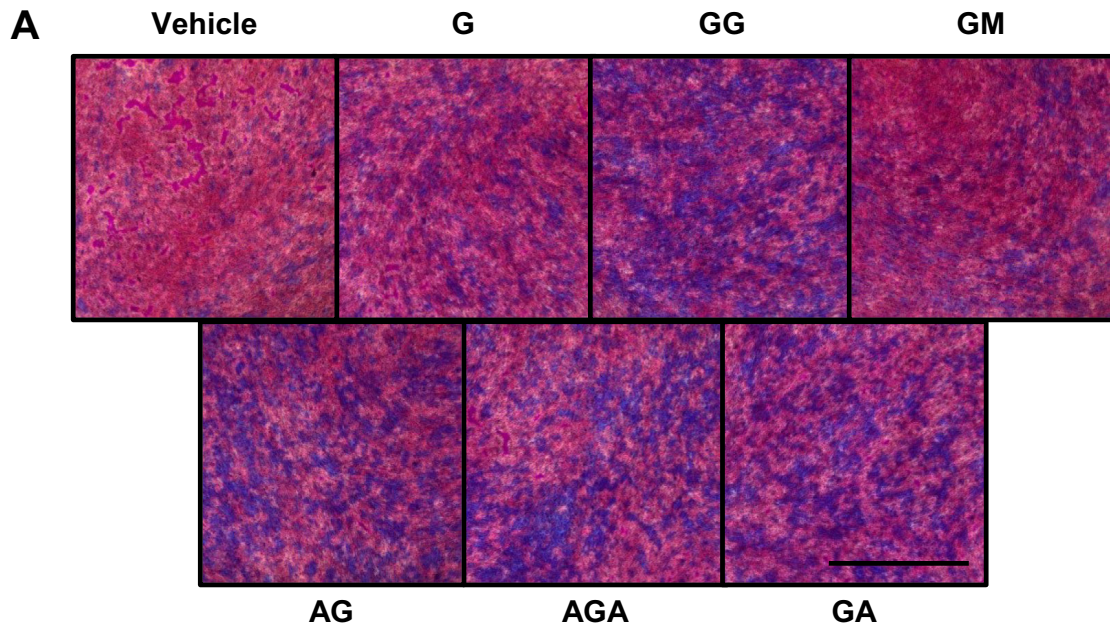
◄**Fig. 1** OSM-induced effects of glycine derivatives on synthesis of collagen and the expression of osteoblast differentiation marker genes in MC3T3-E1 cells. **A** MC3T3-E1 cells were treated with OSM with or without 1 mM of glycine derivatives for 6 days. Collagen deposition was detected using Trichrome staining. Original magnification: × 40. Scale bar, 1 mm. **B** MC3T3-E1 cells were treated with OSM and 1 mM of glycine or glycine derivatives for 4 days. mRNA expression of osteogenesis marker genes *Col1a1*, *Alp*, *Osx*, *Runx2*, *Bsp*, and *Ocn* was quantitatively analyzed using RT-qPCR. Results are presented as fold changes in three independent experiments. *$p < 0.05$, **$p < 0.01$, ***$p < 0.001$ by Student's *t* test. *G* 1 mM glycine, *GG* 1 mM glycylglycine, *GM* 1 mM glycine methyl ester, *AG* acetyl glycine, *AGA* acetyl glycinamide, *GA* 1 mM glycinamide. *OSM* osteogenic medium, *Col1a1* collagen type I alpha 1, *Alp* alkaline phosphatase, *Osx* osterix, *Runx2* runt-related transcription factor 2, *Bsp* bone sialoprotein, *Ocn* osteocalcin, *RT-qPCR* real-time quantitative polymerase chain reaction

GA increased the expression of *ALP* and *OSX* in a concentration-dependent manner by 45.9% and 83.9%, respectively, compared with BMP2 alone. *BSP* expression was also significantly increased by 61.5% and 70.4% with 0.5 and 1 mM GA, respectively, plus BMP2 compared with BMP2 alone (Fig. 3C).

3.3 Cooperative synthesis of collagen and BSP by GA and BMP2 in human BMSCs

Because GA in combination with BMP2 substantially induced the expression of collagen and osteoblast differentiation marker mRNA, we evaluated the effect of GA on the protein levels of COL1 and BSP in human BMSCs. To determine the synergistic expression of COL1 and BSP caused by BMP2 and GA, cells were pretreated with OSM for 3 days and then with BMP2 with glycine or GA in the presence of OSM for 4 more days. When 1 mM GA was combined with BMP2, the levels of COL1 and BSP were significantly increased by 1.72- and 2.2-fold, respectively, compared with that in the control group (BMP2 alone) (Fig. 4A, B). Additionally, immunocytochemistry confirmed that the expression of COL1 induced by 0.5 and 1 mM GA was stronger than that induced by others (Fig. 4C). These results suggest that GA has a stronger synergistic effect with BMP2 on extracellular protein accumulation than BMP2 alone.

3.4 Nanocomplex formation analysis

To understand the enhanced osteogenic activity of GA, the ability of GA to form nanocomplex with proteins was analyzed as these are readily internalized by cells [23, 24]. The nanocomplex formation was assessed using SEM and spectrophotometric methods. Glycine or GA could form nanocomplexes with BSA (Fig. 5A). A higher amount of nanocomplexes at a submicron size was formed by GA plus BSA than by glycine plus BSA. The higher formation rate of the nanocomplex may be due to strong electrostatic interaction between the negatively charged BSA and positively charged GA [A2]. The conformational change of BSA caused by the addition of glycine or GA was measured using CD. BSA exhibited an intense CD spectrum owing to general α-helical structure of BSA, with a double-negative ellipticity at 210 and 220 nm [26, 27]. For the BSA and glycine mixture, the negative CD band slightly changed (Fig. 5B). However, in the CD spectrum of the BSA and GA mixture, the intensity of the negative band due to the α-helical structure was increased by the strong electrostatic interaction between BSA and GA, which promoted the formation of nanocomplexes. Moreover, a difference in the UV–Vis absorption spectra of BSA with glycine or GA was observed to reflect the interactions in BSA plus glycine or BSA plus GA for nanocomplex formation. Addition of GA to a solution of α-MEM and distilled water containing BSA increased a specific peak at 560 nm while but decreased a peak at 430 nm because of the formation of BSA-GA nanocomplexes via electrostatic interaction (Fig. 5C) [27]. However, the changes in the specific peaks were not observed with the addition of glycine to the BSA solution. These results demonstrate that GA enhances the formation of nanocomplexes with protein through electrostatic interactions.

3.5 Synergistic calvarial bone regeneration by GA and BMP2

Having established that the glycine derivative GA harbors a significant synergistic effect with BMP2 on *in vitro* osteoblast differentiation, the effect on *in vivo* bone regeneration was examined in a mouse calvarial defect model. Collagen sponges soaked with glycine or GA in combination with BMP2 were implanted into mice. Eighteen days after surgery, mice were euthanized, and micro-CT analysis of new bone formation showed that the application of glycine or GA induced new bone formation (Fig. 6A). Moreover, combination of glycine or GA with BMP2 more strongly enhanced bone formation, and GA plus BMP2 most notably enhanced bone formation (Fig. 6A). To quantitatively analyze bone regeneration, bone parameters were analyzed (Fig. 6B). Bone volume (BV) of the groups treated with glycine and GA was significantly increased by 4.01- and 5.04-fold, respectively, compared with that in the defect-only group. Although mice treated with BMP2 alone also showed a significant increase in BV, its combination with GA further enhanced this increase by 65% compared with that in the group treated with BMP2 alone. The BV/tissue volume (TV) of the glycine- and GA-treated groups was significantly
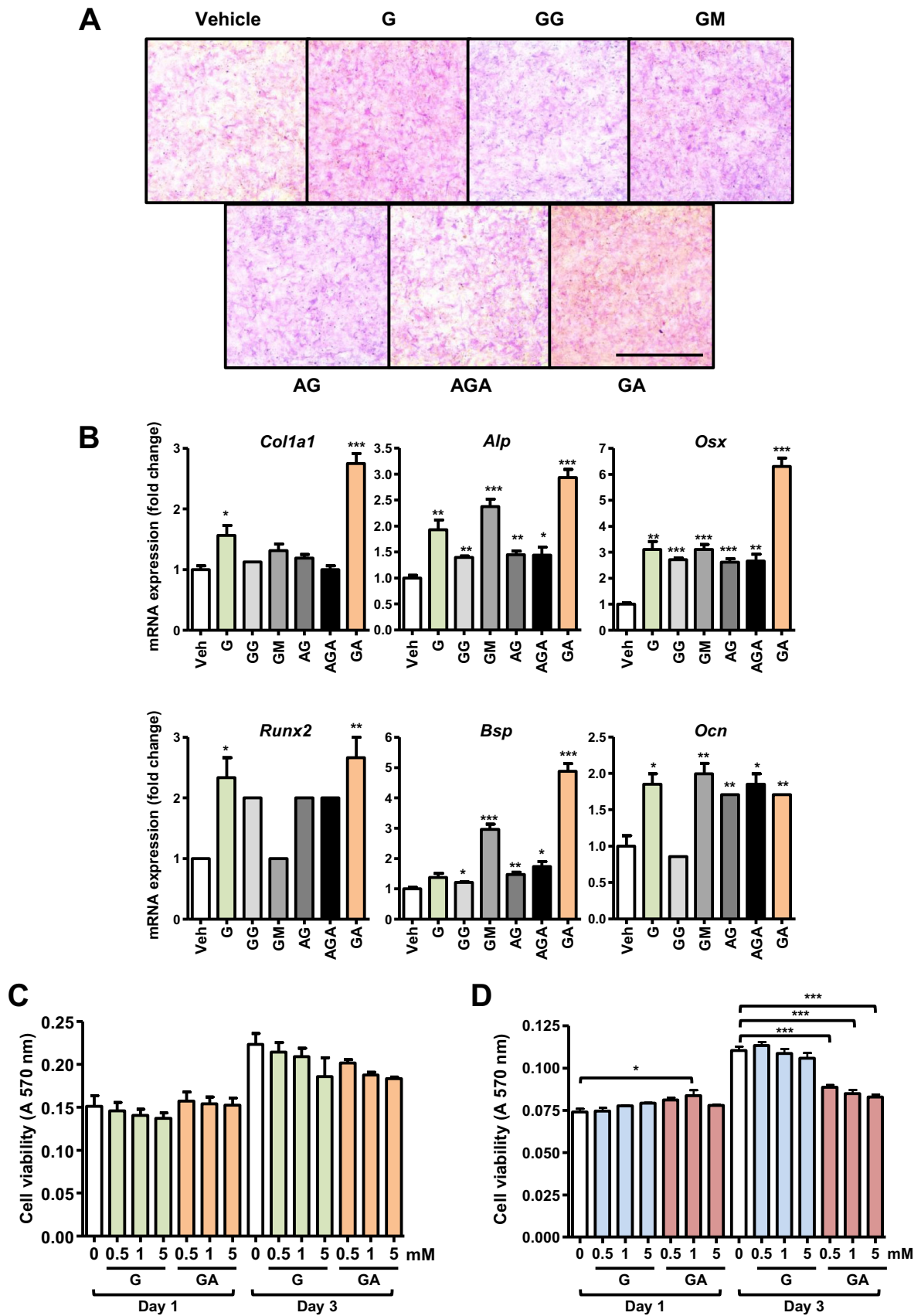
◄ **Fig. 2** Effects of glycine derivatives on activation of ALP and the expression of osteoblast differentiation marker genes by BMP2 in MC3T3-E1 cells. **A** MC3T3-E1 cells were treated with 50 ng/mL of BMP2 with or without 1 mM of glycine derivatives with OSM for 6 days. ALP activity was detected by ALP staining. Original magnification: × 40. Scale bar, 1 mm. **B** MC3T3-E1 cells were treated with 50 ng/mL of BMP2 and 1 mM of glycine or glycine derivatives for 4 days. mRNA expression of osteogenesis marker genes *Col1a1*, *Alp*, *Osx*, *Runx2*, *Bsp*, and *Ocn* was quantitatively analyzed using RT-qPCR. Results are presented as fold changes in three independent experiments. $*p < 0.05$, $**p < 0.01$, $***p < 0.001$ by Student's *t* test. **C, D** Cytotoxicity of glycine derivatives on MC3T3-E1 cells (**C**) and human BMSCs (**D**) were examined using the MTT assay. Data are shown as OD values measured at 570 nm. *G* glycine, *GA* glycinamide. Results are the mean ± standard error of the mean of three independent experiments. Significant differences compared with control (0 mM) were analyzed by one-way ANOVA. *ALP* alkaline phosphatase, *BMP2* bone morphogenetic protein 2, *OSM* osteogenic medium, *Col1a1* collagen type I alpha 1, *Osx* osterix, *Runx2* runt-related transcription factor 2, *Bsp* bone sialoprotein, *Ocn* osteocalcin, *G*, glycine, *GG* glycylglycine, *GM* glycine methyl ester, *AG* acetyl glycine, *AGA* acetyl glycinamide, and *GA* glycinamide, *MTT* 3-(4,5-dimethylthiazol-2-yl)-2,5-diphenyltetrazolium bromide, *OD* optical density, *ANOVA* Analysis of variance

increased by 3.53- and 4.44-fold, respectively, compared with that in the defect-only group. The group treated with BMP2 and GA significantly increased by 64% compared with the group treated with BMP2 alone. Trabecular thickness (Tb.Th) did not significantly differ between groups. The trabecular number (Tb.N) was significantly increased (by 1.6-fold) in the group treated with GA plus BMP2 compared with the group treated with BMP2 alone (Fig. 6B).

The pattern of the calvarial bone regeneration was assessed using histological analysis. H&E staining showed that fibrous tissue was present in the defect-only group (Fig. 6C). A degree of new bone, osteoid, and collagenous fibrous tissue was observed in groups treated with glycine or GA while bone formation was substantially induced in the group treated with BMP2. The groups treated with BMP2 and glycine also demonstrated strongly induced bone formation compared with the group treated with BMP2 alone. BMP2 and GA most strongly induced new bone formation compared with any other groups (Fig. 6C). Histological analysis showed that groups treated with glycine or GA in combination with BMP2 had a significantly increased bone area by 42.8% and 84.7%, respectively, compared with the group treated with BMP2 alone (Fig. 6D). Compared with the glycine plus BMP2 group, the GA plus BMP2 group exhibited significantly increased (by 29%) bone area percentage (Fig. 6D). Trichrome staining was performed to examine the maturity of newly formed bone tissues. The unmineralized new bone area (blue stain) marked with green stars (*) comprised 8.8% and 1.9% in the glycine- and GA-treated groups,

respectively (Fig. 6E). In groups treated with BMP2 alone, glycine plus BMP2, and GA plus BMP2, the immature bone area percentage was 11.7, 28.2, and 21.4%, respectively. Mature bone (red stain) marked with green sharp marks (#) was 8.2% and 10.1% in glycine- and GA-treated groups, respectively. Additionally, in the BMP2 only-, glycine plus BMP2-, and GA plus BMP2-treated groups, the mature bone area percentage was 18.9, 15.5, and 35.2%, respectively. Trichrome staining also showed that the osteoid and mature bone percentages were significantly increased when GA and BMP2 were combined compared with that observed in the other groups (Fig. 6E, F). These results strongly suggest that GA has a synergistic effect with BMP2 for *in vivo* bone regeneration.

4 Discussion

Bone regeneration is fundamentally similar to bone formation during embryonic development and involves the synthesis of major ECM proteins, such as collagen, and the deposition of minerals containing calcium phosphate crystals. The synthesis and expression of collagen requires multiple factors and enzymes [28], and correct control of these processes can promote the generation of ECM proteins that constitute bone. Strategies for enhanced bone regeneration may include applying factors such as transforming growth factor-β and vitamin C to promote the expression of ECM proteins as well as controlling the hydroxylation, glycosylation, crosslinking, and proteolytic cleavage of collagen fibers to promote collagen maturation [28, 29]. Glycine can stimulate collagen synthesis, and in this study, we aimed to identify glycine derivatives that are more potent than glycine in in achieving this aim. Recently, GA has been reported to promote collagen synthesis in dermal fibroblasts [19]. Herein, we screened glycine derivatives and identified several ones that could stimulate collagen synthesis in mouse osteoblast cell lines and human BMSCs. Specifically, GA exhibited the strongest promotion of collagen expression. The protein levels of COL1 and BSP were increased by GA supplementation compared with glycine supplementation, suggesting that GA may have a strong potential to enhance collagen synthesis.

Calcium and phosphate are mineralized and deposited onto the collagen matrix through the action of various proteins [3, 30]. Mineralization occurs during the late stage of osteoblast differentiation and is completed during the formation or regeneration of bone tissue. BMP2 is a potent factor that promotes the differentiation of osteoblasts from mesenchymal stem cells and enhances bone formation. However, because of the various side effects, reducing the BMP dosage is essential for bone regeneration [1, 2]. In
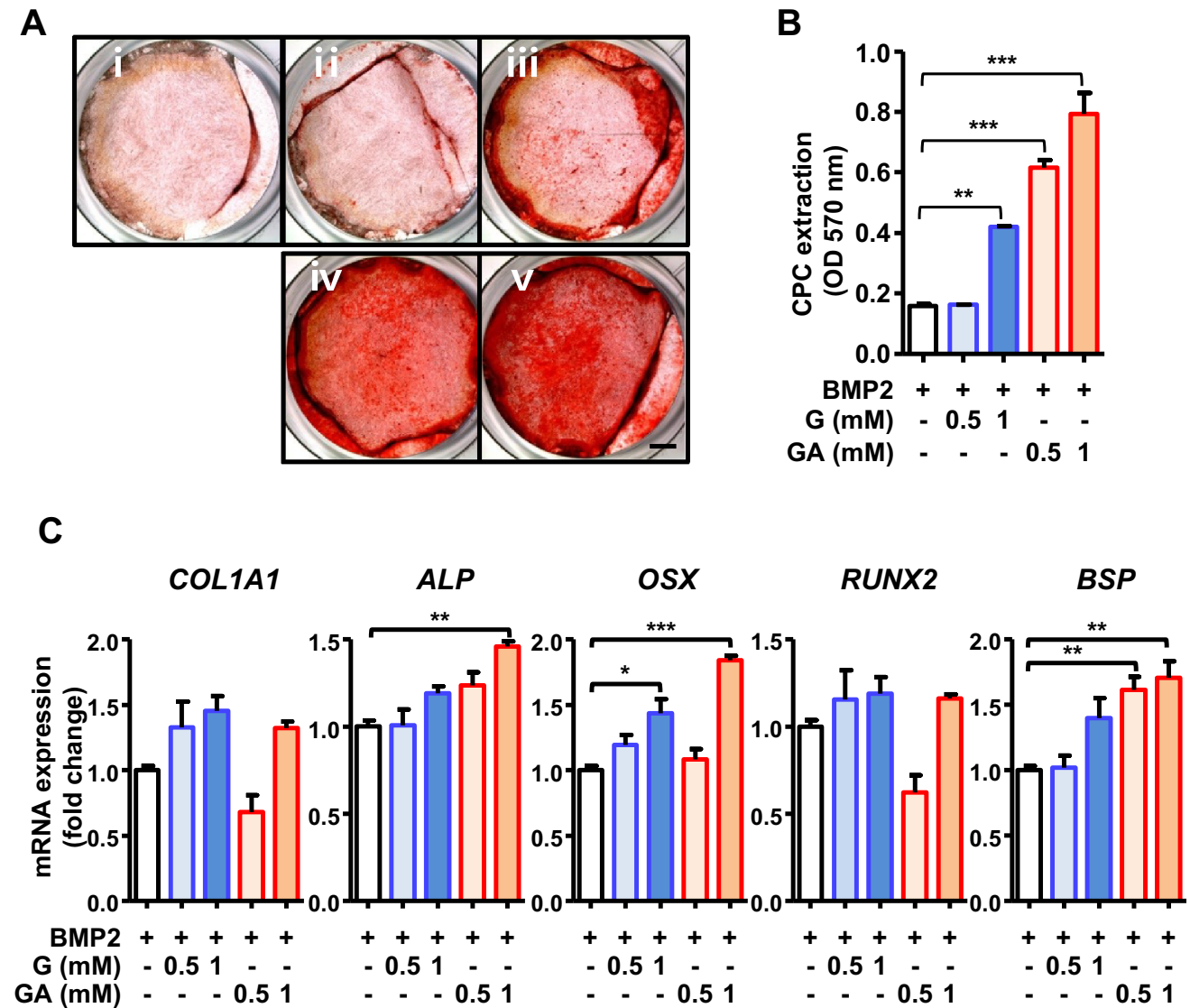
Fig. 3 Effects of glycine and GA on calcium deposition (mineralization) and osteoblast differentiation of human BMSCs *in vitro*. **A** Human BMSCs were pretreated with OSM for 3 days and then treated with 50 ng/mL of BMP2 with or without 0.5 and 1 mM of glycine or GA for 18 days. i: BMP, ii: BMP + 0.5 mM G, iii: BMP + 1 mM G, iv: BMP + 0.5 mM GA, v: BMP + 1 mM GA. Mineralization was detected by Alizarin Red S staining. Original magnification: × 10. Scale bar, 1 mm. **B** Alizarin Red S stain was extracted with CPC for quantifying mineralization. **C** Human BMSCs were pretreated with OSM for 3 days, followed by 50 ng/mL of BMP2 with or without glycine or GA. mRNA expression of osteogenesis marker genes *COL1A1, ALP, OSX, RUNX2,* and *BSP* was analyzed. Results were repeated thrice and presented as fold change. $*p < 0.05$, $**p < 0.01$, $***p < 0.001$ by Student's *t*-test or one-way ANOVA. *G*, glycine; *GA*, glycinamide; *BMP2*, 50 ng/mL of BMP2. *BMSCs* bone marrow mesenchymal stem cells, *ALP* alkaline phosphatase, *BMP2* bone morphogenetic protein 2, *OSM* osteogenic medium, *Col1a1* collagen type I alpha 1, *Osx* osterix, *Runx2* runt-related transcription factor 2, *Bsp* bone sialoprotein

addition to collagen synthesis, GA appeared to promote osteoblast differentiation. Application of BMP2 and GA to human BMSCs synergistically promoted mineralization through calcium deposition. Furthermore, in both mouse osteoblast cell lines and human BMSCs, the expression of osteoblast differentiation markers, such as *RUNX2, ALP, COL1A1, BSP*, and *OSX*, was increased by supplementation with GA and BMP2 compared with supplementation with BMP2 alone or glycine plus BMP2. These results suggest that GA in combination with BMP2 strongly promotes osteoblast differentiation in mouse and human cells.

The cooperative effects of GA and BMP2 on collagen synthesis and osteoblast differentiation can be attributed to the enhancement of BMP signaling pathways. BMP2 binds to BMP receptors and immediately induces multiple signaling pathways including suppressor of mothers against decapentaplegic (SMAD), extracellular signal-regulated kinase (ERK), Jun N-terminal kinase (JNK), and p38
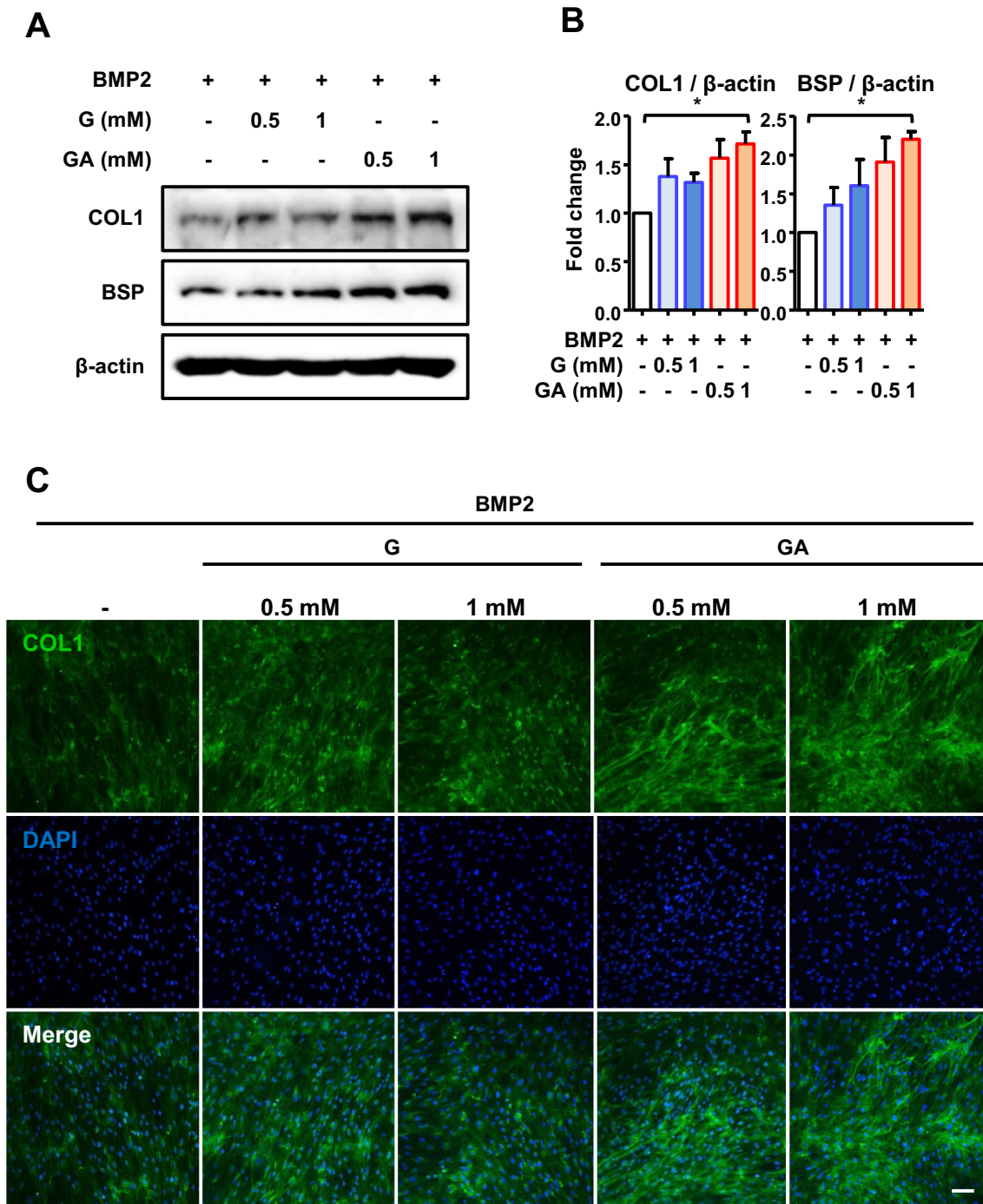
Fig. 4 Effects of glycine and GA on protein levels of COL1 and BSP in human BMSCs. Human BMSCs were pretreated with OSM for 3 days; cells were then treated with 50 ng/mL of BMP2 with or without 0.5 or 1 mM of glycine or GA for 4 days. **A** Effect of glycine or GA on the protein levels of COL1 and BSP in human BMSCs were detected by western blotting. **B** Bands were normalized using ImageJ, and relative expression is shown as fold change compared with control. Results are presented as mean $\pm$ standard error of the mean of three independent experiments. **C** Effect of glycine or GA on COL1 expression was examined using immunocytochemistry. Original magnification: $\times$ 100. Scale bar: 100 μm. *COL1*, collagen type I; *BSP* bone sialoprotein, *BMSCs* bone marrow mesenchymal stem cells, *G* glycine, *GA* glycinamide

mitogen-activated protein kinases (p38) [31, 32], leading to osteoblast differentiation. We consequently assessed the phosphorylation of signaling proteins and showed that the phosphorylation level of SMAD, p38 and ERK was not significantly changed compared with that of signaling molecules induced by BMP2 alone or BMP2 plus glycine
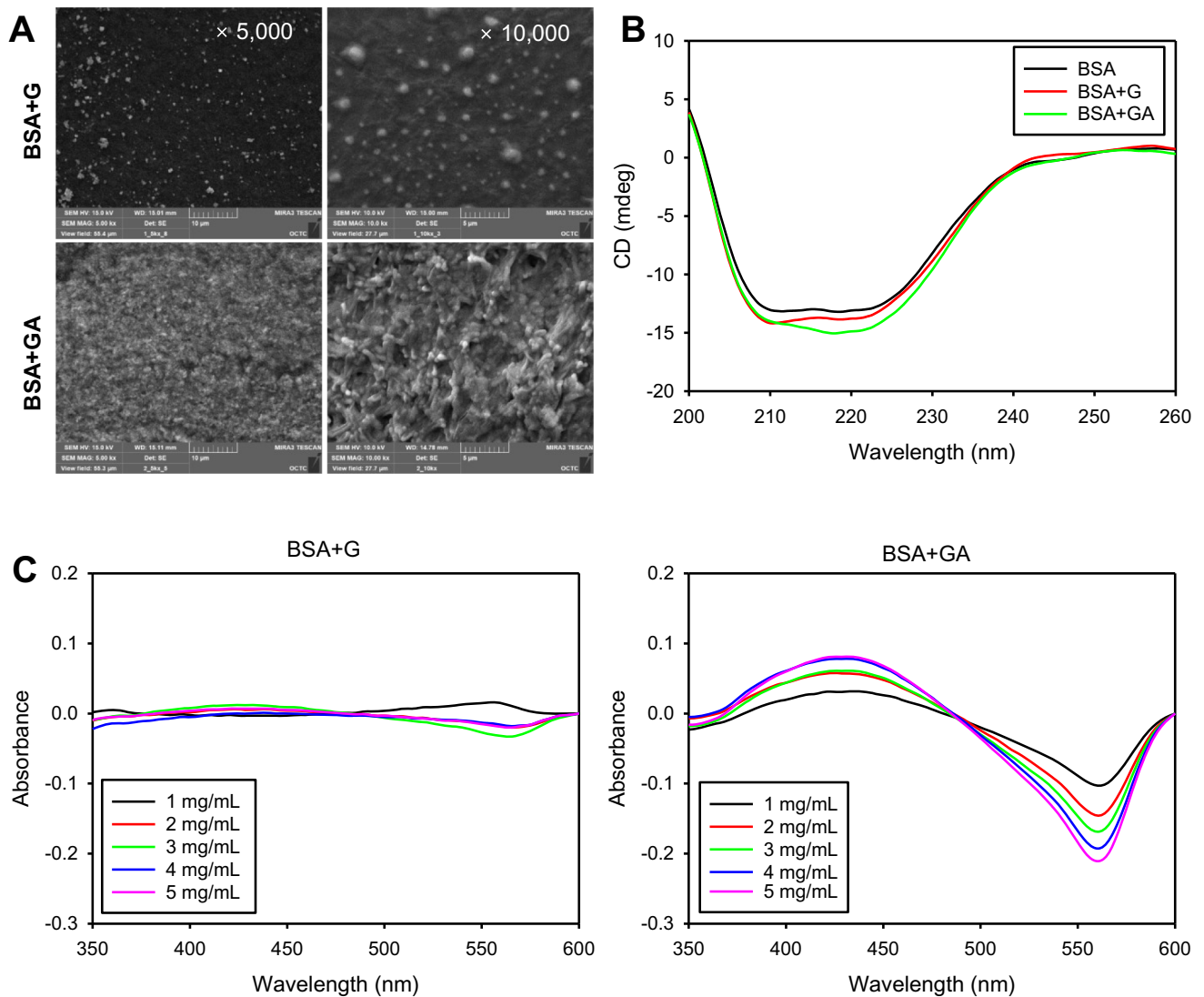
Fig. 5 A SEM images of nanocomplexes formed from BSA plus glycine and BSA plus GA. **B** CD spectra of BSA, BSA plus glycine, and BSA plus GA. **C** Differences in UV–Vis absorption spectra of BSA plus glycine and BSA plus GA with different weight of glycine

or GA. *SEM* scanning electron microscope, *BSA* bovine serum albumin, *G* glycine, *GA* glycinamide, *CD* circular dichroism, *UV*, ultraviolet

(Supplementary Fig. 1). These results indicate that cooperative activation of the immediate early signaling pathway induced by BMP2 and GA does not appear to occur. However, the combination of GA and BMP2 clearly induces the upregulation of protein and mRNA level of collagen and BSP. Moreover, the gene expression of osteoblast differentiation markers *Osx*, *Runx2*, *Alp*, *Col1a1*, and *Bsp* was also further induced by GA plus BMP2 compared with that with BMP alone. The collaborative effect of GA and BMP2 on osteoblast differentiation was also found in human BMSCs. These results suggest that the enhancement of BMP2 plus GA promotes osteoblast differentiation and collagen synthesis in both mouse and human cells.

Therefore, we hypothesized that there might be a more complex and relatively later event such as nanocomplex formation between BMP2 and GA that could promotes cooperative collagen synthesis and osteoblast differentiation. Nanosized particles offer benefits for the delivery of drugs or proteins to target sites via a passive targeting mechanism, thus improving the intracellular uptake of drugs or proteins [23]. Herein, SEM observation showed that the higher amount of nanocomplex formation with GA plus BSA than with glycine plus BSA probably occurred because of the strong electrostatic interaction between the negatively charged amino acids in BSA and positively charged GA. The changes in two negative bands in the UV region of the CD spectra caused by the addition of glycine or GA was attributable to changes in the α-helical structure
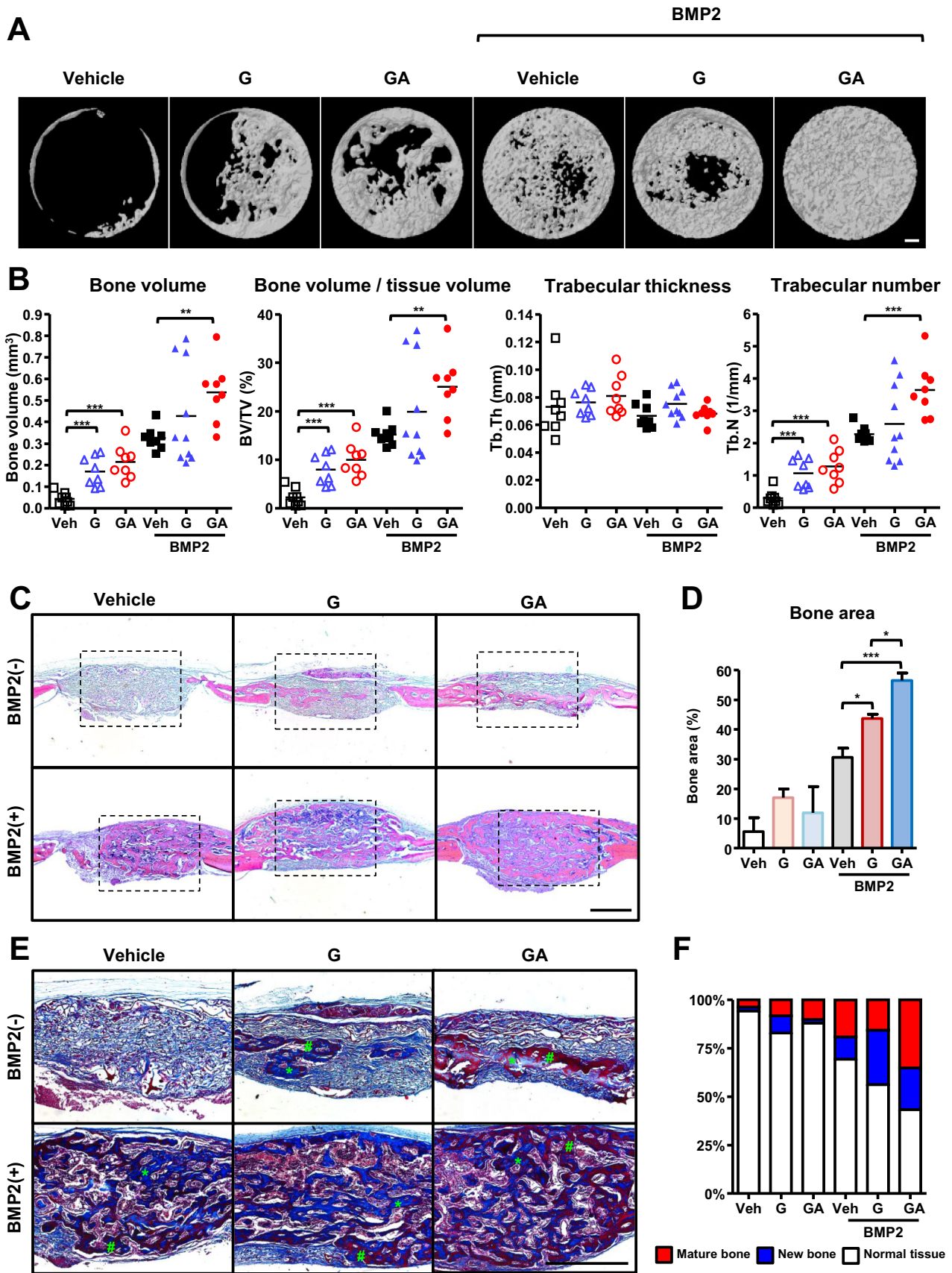
◀**Fig. 6** Effect of glycine and GA on bone regeneration *in vivo*. Mouse calvarial defects were made with a 2-mm diameter and implanted with a collagen sponge soaked in 1 M glycine or GA with or without 0.25 μg BMP2. **A** Three-dimensional reconstructed micro-CT images at 18 days after surgery. Scale bar, 100 μm. **B** Quantitative analysis of bone morphometric parameters, BV, BV/TV, Tb.Th, and Tb.N from newly formed bone at defect site was performed. BV, bone volume; BV/TV, the ratio of mineralized bone volume to the defect tissue volume; Tb.Th, trabecular thickness; Tb.N, trabecular number. **C** H&E-stained images of newly formed bone at defect sites. Original magnification: × 50, Scale bar, 500 μm. **D** Percentage of newly formed bone at defect site. **E** Masson's trichrome stained images at defect sites. **F** Percentage of new or mature bone at specific sites. Green stars; *, Green sharp mark; #. *$p < 0.05$, **$p < 0.01$, ***$p < 0.001$ by Student's *t* test. G, glycine; GA, glycinamide

of BSA and confirmed the formation of nanocomplexes in glycine plus BSA and in GA plus BSA. However, the band intensity of BSA more significantly changed by the addition of GA compared with that following the addition of glycine, which was attributable to changes in the protein secondary structure caused by strong electrostatic interactions. Furthermore, the difference in the UV–Vis spectra of BSA with glycine or GA clearly revealed the enhanced formation of nanocomplexes in GA plus BSA via electrostatic interaction.

The observed collaborative *in vitro* osteogenic effects of GA plus BMP2 were confirmed using an *in vivo* calvarial defect model. Micro-CT evaluation revealed that the GA plus BMP2 group displayed more new bone formation than the BMP2 alone or glycine plus BMP2 groups. The bone morphometric (BV, BV/TV, and Th.N) values for newly formed bone confirmed that GA has a positive effect on bone regeneration. GA further potentiated the bone forming effects of BMP2. Additionally, histological analysis results complemented the micro-CT findings of bone formation within the defect area. These findings are consistent with our hypothesis that local application of GA in combination with BMP2 synergistically promotes bone regeneration. Interestingly, although the mode of action of GA has not been clearly demonstrated, the expression of the receptor for its analog glycine was not changed by GA or glycine supplementation in osteoblasts (data not shown). However, GA clearly affects proliferation retardation, collagen synthesis, and osteoblast differentiation through enhancement of BMP2-mediated signaling pathway activation.

In summary, we demonstrate that GA, which is a component of intermediates in DNA metabolism, stimulates osteoblast differentiation as well as collagen synthesis in murine and human cells. Importantly, when combined with BMP2, GA further enhances *in vitro* collagen synthesis and osteoblast differentiation and *in vivo* regeneration of calvarial bone defects. These results suggest that GA in combination with BMP2 significantly improves the quality of bone regeneration and shortens the duration of regeneration.

Data availability The data are available from the corresponding author upon reasonable request.

Declarations

Conflict of interest The authors declare that they have no competing interests.

Ethical approval The animal study protocol was reviewed and approved by the Committee on the Care and Use of Animals in Research at Kyungpook National University (KNU 2021–0071).

References

1. Krishnakumar GS, Roffi A, Reale D, Kon E, Filardo G. Clinical application of bone morphogenetic proteins for bone healing: a systematic review. Int Orthop. 2017;41:1073–83.
2. James AW, LaChaud G, Shen J, Asatrian G, Nguyen V, Zhang X, et al. A review of the clinical side effects of bone morphogenetic protein-2. Tissue Eng Part B Rev. 2016;22:284–97.
3. Lin X, Patil S, Gao YG, Qian A. The bone extracellular matrix in bone formation and regeneration. Front Pharmacol. 2020;11:757.
4. An J, Yang H, Zhang Q, Liu C, Zhao J, Zhang L, et al. Natural products for treatment of osteoporosis: the effects and mechanisms on promoting osteoblast-mediated bone formation. Life Sci. 2016;147:46–58.
5. Fernandez-Tresguerres-Hernandez-Gil I, Alobera-Gracia MA, del Canto-Pingarron M, Blanco-Jerez L. Physiological bases of bone regeneration II. The remodeling process. Med Oral Patol Oral Cir Bucal. 2016;11:E151-7.
6. Young MF. Bone matrix proteins: more than markers. Calcif Tissue Int. 2003;72:2–4.
7. Diegelmann RF. Collagen metabolism. Wounds. 2001;13:177–82.
8. Shoulders MD, Raines RT. Collagen structure and stability. Annu Rev Biochem. 2009;78:929–58.
9. Bowes JH, Kenten RH. The amino-acid composition and titration curve of collagen. Biochem J. 1948;43:358–65.
10. Pauling L, Corey RB. The structure of fibrous proteins of the collagen-gelatin group. Proc Natl Acad Sci. 1951;37:272–81.
11. Moreira PL, An YH, Santos AR Jr, Genari SC. In vitro analysis of anionic collagen scaffolds for bone repair. J Biomed Mater Res B Appl Biomater. 2004;71:229–37.

12. Tsuji N, Yoshikawa M, Shimomura Y, Yabuuchi T, Hayashi H, Ohgushi H. Osteogenic influence of lysine in porous hydroxyapatite scaffold. Key Eng Mater. 2008;361–363:1189–92.

13. Park SH, Gil ES, Kim HJ, Lee K, Kaplan DL. Relationships between degradability of silk scaffolds and osteogenesis. Biomaterials. 2010;31:6162–72.

14. Long CG, Braswell E, Zhu D, Apigo J, Baum J, Brodsky B. Characterization of collagen-like peptides containing interruptions in the repeating Gly-X-Y sequence. Biochemistry. 1993;32:11688–95.

15. de Paz-Lugo P, Lupianez JA, Melendez-Hevia E. High glycine concentration increases collagen synthesis by articular chondrocytes in vitro: acute glycine deficiency could be an important cause of osteoarthritis. Amino Acids. 2018;50:1357–65.

16. Kim MH, Kim HM, Jeong HJ. Estrogen-like osteoprotective effects of glycine in in vitro and in vivo models of menopause. Amino Acids. 2016;48:791–800.

17. Kim JH, Seok JK, Kim YM, Boo YC. Identification of small peptides and glycinamide that inhibit melanin synthesis using a positional scanning synthetic peptide combinatorial library. Br J Dermatol. 2019;181:128–37.

18. Boo YC, Jo DJ, Oh CM, Lee SY, Kim YM. The first human clinical trial on the skin depigmentation efficacy of glycinamide hydrochloride. Biomedicines. 2020;8:257.

19. Boo YC. Ascorbic acid (vitamin c) as a cosmeceutical to increase dermal collagen for skin antiaging purposes: emerging combination therapies. Antioxidants (Basel). 2022;11:1663.

20. Zhu M, Zhao SC, Xin C, Zhu YF, Zhang CQ. 3D-printed dimethyloxallyl glycine delivery scaffolds to improve angiogenesis and osteogenesis. Biomater Sci. 2015;3:1236–44.

21. Shang LL, Liu ZQ, Ma BJ, Shao JL, Wang B, Ma CX, et al. Dimethyloxallyl glycine/nanosilicates-loaded osteogenic/angiogenic difunctional fibrous structure for functional periodontal tissue regeneration. Bioact Mater. 2021;6:1175–88.

22. Qi X, Liu Y, Ding ZY, Cao JQ, Huang JH, Zhang JY, et al. Synergistic effects of dimethyloxallyl glycine and recombinant human bone morphogenetic protein-2 on repair of critical-sized bone defects in rats. Sci Rep. 2017;7:42820.

23. Seong DY, Kim YJ. Enhanced photodynamic therapy efficacy of methylene blue-loaded calcium phosphate nanoparticles. J Photochem Photobiol B. 2015;146:34–43.

24. Kim MG, Kang TW, Park JY, Park SH, Ji YB, Ju HJ, et al. An injectable cationic hydrogel electrostatically interacted with BMP2 to enhance in vivo osteogenic differentiation of human turbinate mesenchymal stem cells. Mater Sci Eng C Mater Biol Appl. 2019;103:109853.

25. Hong YR, Kim TH, Park KH, Kang J, Lee K, Park EK, et al. rhBMP-2-Conjugated three-dimensional-printed poly(L-lactide) scaffold is an effective bone substitute. Tissue Eng Regen Med. 2023;20:69–81.

26. Pang JY, Sha XF, Chao YH, Chen GY, Han CR, Zhu WS, et al. Green aqueous biphasic systems containing deep eutectic solvents and sodium salts for the extraction of protein. RSC Adv. 2017;7:49361–7.

27. Paul S, Sepay N, Sarkar S, Roy P, Dasgupt S, Sardar PS, et al. Interaction of serum albumins with fluorescent ligand 4-azido coumarin: spectroscopic analysis and molecular docking studies. New J Chem. 2017;41:15392–404.

28. Ray S, Adelnia H, Ta HT. Collagen and the effect of poly-l-lactic acid based materials on its synthesis. Biomater Sci. 2021;9:5714–31.

29. Salo AM, Myllyharju J. Prolyl and lysyl hydroxylases in collagen synthesis. Exp Dermatol. 2021;30:38–49.

30. Murshed M. Mechanism of bone mineralization. Cold Spring Harb Perspect Med. 2018;8:a031229.

31. Lai CF, Cheng SL. Signal transductions induced by bone morphogenetic protein-2 and transforming growth factor-beta in normal human osteoblastic cells. J Biol Chem. 2002;277:15514–22.

32. Rodriguez-Carballo E, Gamez B, Ventura F. p38 MAPK signaling in osteoblast differentiation. Front Cell Dev Biol. 2016;4:40.